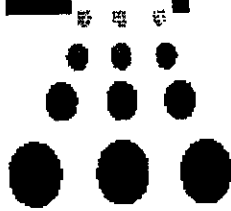




# Jefferson Lab PAC13 Proposal Cover Sheet

This document must be received by close of business Thursday, **December 18, 1997** at:

Jefferson Lab  
User Liaison Office,  
Mail Stop 12B  
12000 Jefferson Avenue  
Newport News, VA  
23606



Experimental Hall:     A      
Days Requested for Approval:     12    

- New Proposal Title:** Systematic Probe of Short-Range Correlations via the Reaction  ${}^4\text{He}(e, e'p){}^3\text{H}$ .
  - Update Experiment Number:**
  - Letter-of-Intent Title:**
- (Choose one)

### Proposal Physics Goals

Indicate any experiments that have physics goals similar to those in your proposal.

Approved, Conditionally Approved, and/or Deferred Experiment(s) or proposals:

89-044, 97-006, 97-011, Mainz A1/3-96

### Contact Person

**Name:** Jeff Templon  
**Institution:** University of Georgia  
**Address:** Department of Physics and Astronomy  
**Address:** Cedar Street and Sanford Drive/Physics Building  
**City, State, ZIP/Country:** Athens, Georgia, 30602-2451, U.S.A.  
**Phone:** 706/542-2843      **Fax:** 706/542-2492  
**E-Mail:** templon@cebaf.gov

Receipt Date: 12/18/97

JLab Use Only

PR 97-111

By:     JP

# BEAM REQUIREMENTS LIST

JLab Proposal No.: \_\_\_\_\_ Date: 12/16/97

Hall: A Anticipated Run Date: \_\_\_\_\_ PAC Approved Days: \_\_\_\_\_

Spokesperson: Jeff Templon

Hall Liaison: J.P. Chen

Phone: 706/542-2843

E-mail: templon@cebaf.gov

List all combinations of anticipated targets and beam conditions required to execute the experiment. (This list will form the primary basis for the Radiation Safety Assessment Document (RSAD) calculations that must be performed for each experiment.)

Condition No.	Beam Energy (MeV)	Mean Beam Current ( $\mu$ A)	Polarization and Other Special Requirements (e.g., time structure)	Target Material (use multiple rows for complex targets — e.g., w/windows)	Material Thickness (mg/cm <sup>2</sup> )	Est. Beam-On Time for Cond. No. (hours)
1	4045	20		<sup>1</sup> H	2100	3
2	4045	20		<sup>4</sup> He	1525	2
3	4045	100		<sup>4</sup> He	1525	45
4	4045	100		<sup>4</sup> He	1525	133
5	2445	20		<sup>1</sup> H	2100	3
6	2445	100		<sup>4</sup> He	1525	27.5
7	3245	20		<sup>1</sup> H	2100	3
8	3245	100		<sup>4</sup> He	1525	41.5

The beam energies,  $E_{\text{Beam}}$ , available are:  $E_{\text{Beam}} = N \times E_{\text{Linac}}$  where  $N = 1, 2, 3, 4, \text{ or } 5$ .  $E_{\text{Linac}} = 800$  MeV, i.e., available  $E_{\text{Beam}}$  are 800, 1600, 2400, 3200, and 4000 MeV. Other energies should be arranged with the Hall Leader before listing.

# HAZARD IDENTIFICATION CHECKLIST

JLab Proposal No.: \_\_\_\_\_

Date: 12/15/97

(For CEBAF User Liaison Office use only.)

NOTE: Where not marked, all equipment is standard Hall A setup.

Check all items for which there is an anticipated need.

<p><b>Cryogenics</b></p> <p>_____ beamline magnets</p> <p>_____ analysis magnets</p> <p><input checked="" type="checkbox"/> target</p> <p>type: <u>helium</u></p> <p>flow rate: _____</p> <p>capacity: _____</p>	<p><b>Electrical Equipment</b></p> <p>_____ cryo/electrical devices</p> <p>_____ capacitor banks</p> <p>_____ high voltage</p> <p>_____ exposed equipment</p>	<p><b>Radioactive/Hazardous Materials</b></p> <p>List any radioactive or hazardous/toxic materials planned for use:</p> <p>_____</p> <p>_____</p> <p>_____</p>
<p><b>Pressure Vessels</b></p> <p>_____ inside diameter</p> <p>_____ operating pressure</p> <p>_____ window material</p> <p>_____ window thickness</p>	<p><b>Flammable Gas or Liquids</b></p> <p>type: _____</p> <p>flow rate: _____</p> <p>capacity: _____</p> <p><b>Drift Chambers</b></p> <p>type: _____</p> <p>flow rate: _____</p> <p>capacity: _____</p>	<p><b>Other Target Materials</b></p> <p>_____ Beryllium (Be)</p> <p>_____ Lithium (Li)</p> <p>_____ Mercury (Hg)</p> <p>_____ Lead (Pb)</p> <p>_____ Tungsten (W)</p> <p>_____ Uranium (U)</p> <p>_____ Other (list below)</p> <p>_____</p> <p>_____</p>
<p><b>Vacuum Vessels</b></p> <p>_____ inside diameter</p> <p>_____ operating pressure</p> <p>_____ window material</p> <p>_____ window thickness</p>	<p><b>Radioactive Sources</b></p> <p>_____ permanent installation</p> <p>_____ temporary use</p> <p>type: _____</p> <p>strength: _____</p>	<p><b>Large Mech. Structure/System</b></p> <p>_____ lifting devices</p> <p>_____ motion controllers</p> <p>_____ scaffolding or</p> <p>_____ elevated platforms</p>
<p><b>Lasers</b></p> <p>type: _____</p> <p>wattage: _____</p> <p>class: _____</p> <p>Installation:</p> <p>_____ permanent</p> <p>_____ temporary</p> <p>Use:</p> <p>_____ calibration</p> <p>_____ alignment</p>	<p><b>Hazardous Materials</b></p> <p>_____ cyanide plating materials</p> <p>_____ scintillation oil (from)</p> <p>_____ PCBs</p> <p>_____ methane</p> <p>_____ TMAE</p> <p>_____ TEA</p> <p>_____ photographic developers</p> <p>_____ other (list below)</p> <p>_____</p> <p>_____</p>	<p><b>General:</b></p> <p>Experiment Class:</p> <p><input checked="" type="checkbox"/> Base Equipment</p> <p>_____ Temp. Mod. to Base Equip.</p> <p>_____ Permanent Mod. to Base Equipment</p> <p>_____ Major New Apparatus</p> <p>Other: <u>high-power</u></p> <p><u>helium target</u></p>

# LAB RESOURCES LIST

JLab Proposal No.: \_\_\_\_\_

Date 12/15/97

*(For JLab ULO use only.)*

List below significant resources — both equipment and human — that you are requesting from Jefferson Lab in support of mounting and executing the proposed experiment. Do not include items that will be routinely supplied to all running experiments such as the base equipment for the hall and technical support for routine operation, installation, and maintenance.

## Major Installations *(either your equip. or new equip. requested from JLab)*

High-power Helium Target

\_\_\_\_\_

\_\_\_\_\_

\_\_\_\_\_

\_\_\_\_\_

*New Support Structures:* \_\_\_\_\_

\_\_\_\_\_

\_\_\_\_\_

## Data Acquisition/Reduction

*Computing Resources:* \_\_\_\_\_

Standard

\_\_\_\_\_

\_\_\_\_\_

*New Software:* \_\_\_\_\_

Standard

\_\_\_\_\_

\_\_\_\_\_

## Major Equipment

Magnets: Standard

\_\_\_\_\_

Power Supplies: Standard

\_\_\_\_\_

Targets: High-Power Helium Cryotarget

\_\_\_\_\_

Detectors: Standard

\_\_\_\_\_

Electronics: Standard

\_\_\_\_\_

Computer Hardware: Standard

\_\_\_\_\_

Other: Sieve Slit in Spectrometer

\_\_\_\_\_

Other: \_\_\_\_\_

\_\_\_\_\_

\_\_\_\_\_

\_\_\_\_\_

# Systematic Probe of Short-Range Correlations *via* the Reaction ${}^4\text{He}(e, e'p){}^3\text{H}$

Proposal to the Jefferson Lab PAC, December 1997

J. A. Templon, F. T. Baker, J. Hines  
*The University of Georgia, Athens, GA*  
J. P. Chen, J. H. Mitchell, J. J. LeRose  
*Thomas Jefferson National Accelerator Facility*  
A. Sarty  
*Florida State University, Tallahassee, FL*  
E. Jans and L. Lapikás  
*NIKHEF, Amsterdam, The Netherlands*  
M. Epstein  
*California State University at Los Angeles*  
M. Sargsian  
*Technische Universität München, Germany and*  
*Yerevan Physics Institute, Armenia*  
L. L. Howell and S. A. Sofianos  
*University of South Africa, Pretoria*

## Hall A Collaboration Proposal

December 18, 1997

### Abstract

We propose to measure unseparated cross sections for the reaction  ${}^4\text{He}(e, e'p){}^3\text{H}$  in several different types of kinematics. In each

kinematical setting, measurements will be made over the recoil momentum region 350–550 MeV/ $c$ , which spans the first minimum and second maximum predicted in the  $t + p$  overlap function. The location of the minimum and the height of the second maximum are determined by the short-range part of the  $NN$  interaction. Experiments performed so far have not observed any corresponding structures. Of equal importance are the various kinematical settings in which we propose to study this recoil-momentum range; they reflect different ideas from theory about how to suppress final-state interactions and meson-exchange currents. Calculations blame these effects for obscuring these SRC signatures in previous experiments.

## 1 Introduction

A convincing demonstration of short range correlations remains an elusive goal of  $(e, e'p)$  studies [1]. One set of experiments [2, 3, 4] has tried to find it in cross sections for valence proton knockout at large recoil momentum; comparison with theory shows sizeable effects of long-range correlations, but little effect of short-range correlations. Another set [5, 6, 7, 8, 9] has focussed on the region where both the recoil momentum and missing energy are large. A convincing signature of a two-body knockout mechanism was observed, but one must rely on theoretical calculations to understand how to separate the part due to short-range correlations from contributions from two-body currents such as  $\Delta$  excitation and meson-exchange currents.

We propose to measure the reaction  ${}^4\text{He}(e, e'p){}^3\text{H}$  (the two-body breakup channel) as an alternate means to observe effects of short-range correlations. Tadokoro *et al* [10] have calculated that the spectral function for  ${}^4\text{He} \rightarrow t + p$  has a shape which can be related directly to short-range correlations. Realistic calculations of this spectral function presented in [10] as well as in [11, 12] are shaped similar to a classical diffraction pattern, with the first minimum somewhere near 430 MeV/ $c$  and the second maximum at around 530 MeV/ $c$ .

The calculations of this spectral function from [10] are displayed in Fig. 1. The curve which drops monotonically towards zero was calculated using an independent-particle (harmonic oscillator) nuclear model, while the others were computed using realistic  $NN$  interactions, including two-body correlations *via* the ATMS method [13]. One can easily see that the diffractive pattern comes from something which is missing in the independent-particle

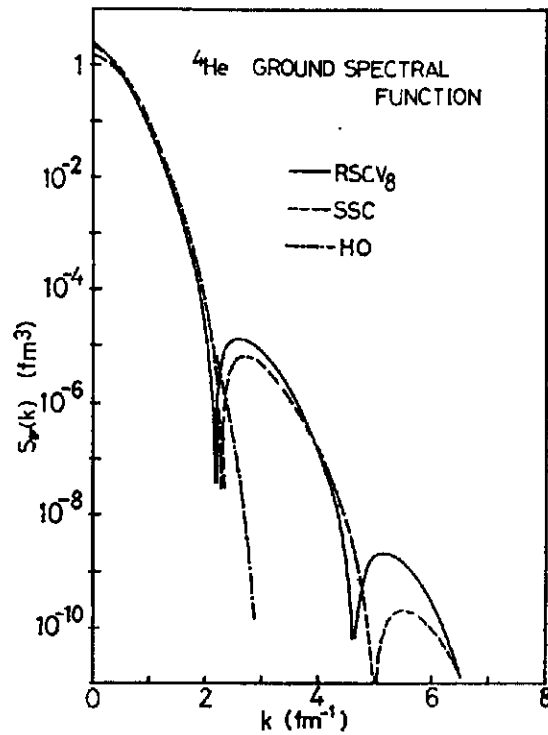


Figure 1: Spectral functions for  ${}^4\text{He} \rightarrow t + p$  calculated using various  $NN$  potential models. The dot-dashed curve (which falls monotonically) was calculated using an independent-particle (harmonic-oscillator) model. This figure is reprinted from [10].

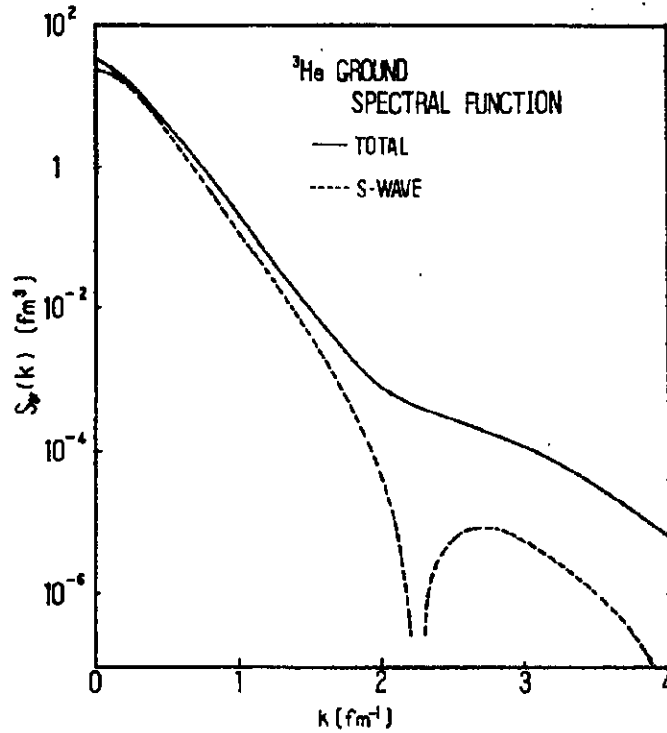


Figure 2: The spectral function for  ${}^3\text{He} \rightarrow d + p$ . The solid curve is a full calculation, and the dashed curve shows the result if the  $d$ -wave part of the  $d + p$  wavefunction is neglected. This figure is reprinted from [10].

model, which lacks short-range correlations.

Fig. 2 shows the corresponding spectral function for  ${}^3\text{He}$  ( ${}^3\text{He} \rightarrow d + p$ ). This curve is monotonic, which raises the question, “why are  ${}^3\text{He}$  and  ${}^4\text{He}$  so different?” Takodoro *et al* argue that the contributions from  $d$ -state components in the wavefunctions are responsible. The dashed curve in Fig. 2 shows only the  $s$ -wave contribution, which is similar to the full calculation for  ${}^4\text{He}$ . It is further observed that it is not possible to couple a proton and a triton, in a relative  $L = 2$  state, to the  $J^\pi = 0^+$   ${}^4\text{He}$  ground state.

Coupling this observation with those from Fig. 1, it is concluded that the structure seen in  $n_{tp}(k)$  for  ${}^4\text{He}$  at high  $k$  is directly linked to  $s$ -wave SRC in the ground state. In particular, the location of the minimum and the height of the second maximum are sensitive to the  $NN$  potential model used (see



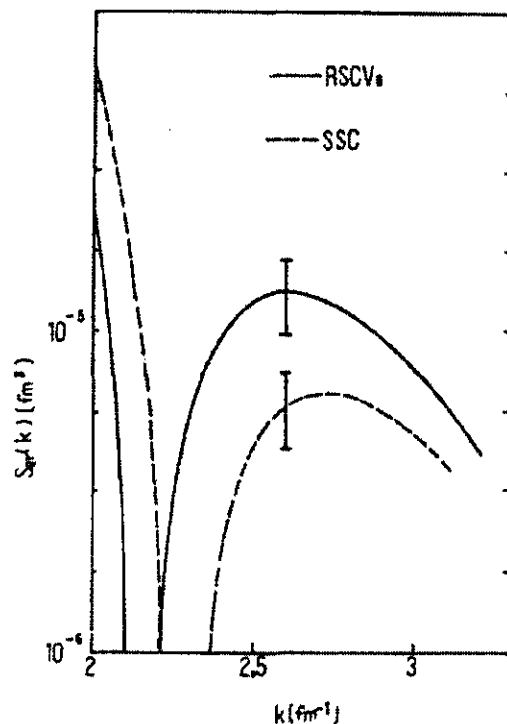


Figure 3: Expanded view of the region around the second maximum in the spectral function  ${}^4\text{He} \rightarrow t + p$ . The two curves correspond to two different  $NN$  potential models. This figure is reprinted from [10].

Fig. 3), which presumably at such high momenta can only reflect differences in the short-range structure calculated in the various models. The absence of  $d$ -wave contributions is fortuitous, since the longer-ranged tensor correlations are strong in the  $d$ -wave channel.

It is well known that to first order, an  $(e, e'p)$  cross section is proportional to the hole spectral function. Thus a measurement of the cross section in the appropriate kinematics would be a direct probe of the short-range correlations in  ${}^4\text{He}$ . Problems arise since the world is not plane wave in nature, and the impulse approximation is not perfect. The effects above plane wave (final-state interactions, isobar currents, and meson exchange currents) are relatively amplified in the region we wish to probe, since we are measuring in a region where the PWIA part of the cross section goes through a minimum.

Section 2 discusses previous measurements that are similar in spirit to the

one being proposed. These experiments did not observe significant signatures of the predicted structure. Section 3 discusses ideas that have been put forward about how to suppress the contaminant processes and afford a more direct measure of the hole spectral function. Section 4 discusses what we plan to measure. The proposed plan has the attractive feature of testing much of the  $(e, e'p)$  folklore on how MEC and FSI should behave in various kinematic regions. Section 6 discusses experimental considerations such as equipment and beam-time allocations. Finally, we discuss the relation of the current proposal to other approved experiments at Jefferson Lab and elsewhere.

## 2 Previous Experiments

Two experiments [8, 9, 14] have measured the cross section for  ${}^4\text{He}(e, e'p){}^3\text{H}$  at recoil momenta covering the range of interest (350–550 MeV/ $c$ ). Neither of these experiments observed a significant signature of the dip near 450 MeV/ $c$ . The data of [8] are somewhat questionable, since theoretical calculations disagree by more than a factor of two with these data, even at lower recoil momentum where the same calculation agrees with other experiments [9, 15, 16, 17, 18]. The results of [14] are qualitatively similar to those of [9], thus we restrict a detailed discussion to the data from the latter experiment.

The data are shown in Fig. 4 along with calculations by Laget [19], Schiavilla [20], and Nagorny [21, 22]. A keen eye (or a good imagination) is necessary to discern any inflection in the data at the location where the PWIA (dotted curves) predicts the zero. One can see the dependence of the zero position on the  $NN$  interaction model in these PWIA curves; Schiavilla and Laget both used wavefunctions obtained with the Argonne v14  $NN$  potential and Urbana model-VII  $3N$  interaction, while Nagorny obtained wavefunctions using the Argonne v18  $NN$  interaction and Urbana model-IX  $3N$  force. According to the calculations, the minimum is not observed due to the combined effects of FSI (the dashed curves in panels a) and b) of Fig. 4) and MEC (the full curves include both MEC and FSI).

These data (taken at NIKHEF) were measured by fixing the electron kinematics so that  $(\omega, |\vec{q}|)$  were (215 MeV, 400 MeV/ $c$ ) respectively. The recoil momentum  $p_m$  was varied by simply changing the proton emission angle. For  $p_m = 450$  MeV/ $c$ , the emission angle was such that  $\theta_{pq}$ , the angle between the outgoing proton and  $\vec{q}$ , was about 50 degrees. Previous studies

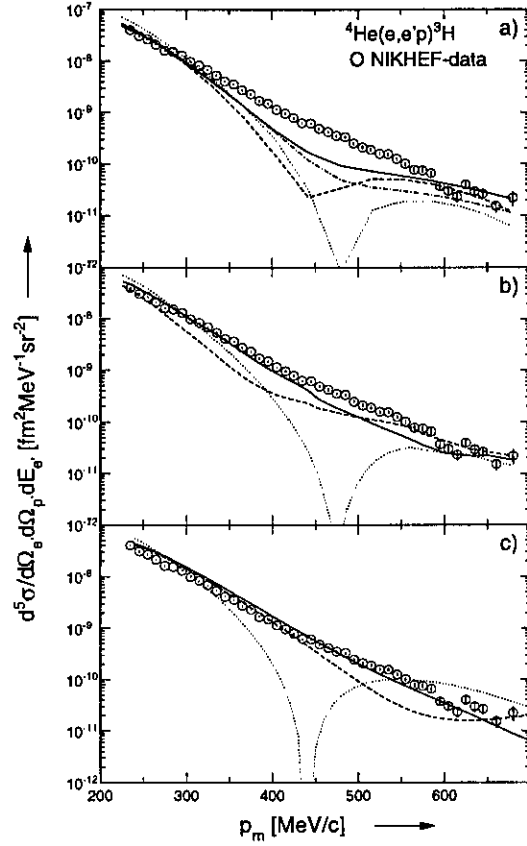


Figure 4: Cross sections for  ${}^4\text{He}(e, e'p){}^3\text{H}$  measured at NIKHEF. Each panel shows the same data compared to a different theoretical calculation. The top figure shows calculations by Laget; the middle panel, by Schiavilla; and the bottom panel, by Nagorny. The solid curves are the full calculations, and the dotted curves are the PWIA results. The dashed curves include distortions, but not MEC effects.

have shown (*e.g.*, [23]) that the cross sections for valence-proton knockout are dominated by FSI effects when one moves away from parallel kinematics. It is in this respect not surprising that FSI effects obscure the minimum for the NIKHEF experiment.

### 3 Suppressing MEC and FSI in $(e, e'p)$ Experiments

The calculations shown in the previous section indicate that both FSI and MEC conspire to wash out the minimum of  $\sigma(p_m)$ . There are many ideas in circulation about how to suppress these effects, most of them being poorly tested at present. Jefferson Lab provides beams with enough energy that these ideas can now be fully tested and exploited.

A word about conventions: we use here  $\vec{p}_m = \vec{p}_f - \vec{q}$ , where  $\vec{p}_f$  is the momentum of the detected proton. In the PWIA,  $\vec{p}_m = \vec{p}_s$ , the momentum of the “struck” nucleon before collision. When referring to the magnitude of the struck-nucleon momentum, we use  $p_m$  since that is the measured quantity. Also, we generally just use the word “minimum” to refer to the predicted minimum and adjacent second maximum in the spectral function  $n_{tp}(k)$  for  ${}^4\text{He}$ . If we don’t observe a minimum, it is difficult to make defensible statements about the height of the second maximum.

#### 3.1 Higher Momentum Transfers

The NIKHEF experiment was done with a central momentum transfer  $q$  of 400 MeV/ $c$ . Close to the quasielastic peak,  $q$  essentially determines the outgoing proton momentum. It is well known from proton-scattering experiments that FSI is a strong function of energy. It is at its lowest at a proton momentum of about 700 MeV/ $c$ . Above this momentum, absorption effects begin to increase, but the elastic rescattering continues to decrease. These behaviours are easily seen by examining the total and elastic  $NN$  cross sections. In this proposal we are interested in the two-body breakup case, so suppression of elastic rescattering is the likely the most important consideration, unless processes like  $\pi$  emission and reabsorption into the elastic channel become important. Unfortunately such calculations are not readily available.

Higher  $q$  would appear to be better, in terms of suppressing FSI, since higher  $q$  generally leads to higher outgoing proton energy.

### 3.2 Parallel Kinematics

The dominance of FSI away from parallel kinematics has been demonstrated by calculation [23]. This dominance can be anticipated by a simple argument. In plane-wave approximation for the hadronic final state, the electron kinematics determine a parameter  $y$  which is the minimum momentum a struck proton could have originally had while still satisfying the measured  $(e, e')$  kinematics. This minimum-momentum situation coincides with parallel kinematics, which means that unscattered nucleons knocked out at nonzero angle with respect to  $\vec{q}$  had initial momenta higher than those along  $\vec{q}$ . In most cases of interest, the spectral function is dropping precipitously with increasing initial momentum, so it is not unlikely that rescattering of the “parallel”, low-initial-momentum nucleons makes a larger contribution to the cross section than does the unscattered, higher-initial-momentum nucleon contribution at the same angle.

A more quantitative demonstration of this behaviour comes from recent eikonal-approximation calculations using a Feynman-diagram approach [24]. They find that FSI modify proton-momentum components transverse to  $\vec{q}$  more strongly than they do those parallel to  $\vec{q}$ . The RMS transverse momentum transfer in rescattering was found to be about 300 MeV/ $c$ , which is another way of saying that if one relies on quasiperpendicular kinematics to reach a given  $p_m$ , FSI can strongly modify the cross section.

This is shown graphically in Fig. 5, where the cross sections for kinematics similar to those being proposed here are calculated within the Generalized Eikonal Approach (GEA) [24]. The  ${}^4\text{He}(e, e'p){}^3\text{H}$  cross section is plotted vs  $p_m$  for parallel, perpendicular, and antiparallel kinematics. The structure of the PWIA (dashed curves) is best retained by the full calculation (solid curves) for parallel kinematics, and is reasonably preserved in antiparallel kinematics. For perpendicular kinematics (when the struck nucleon was travelling perpendicular to  $\vec{q}$ ), the PWIA structure is almost completely eradicated for  $p_m \geq 300$  MeV/ $c$ .

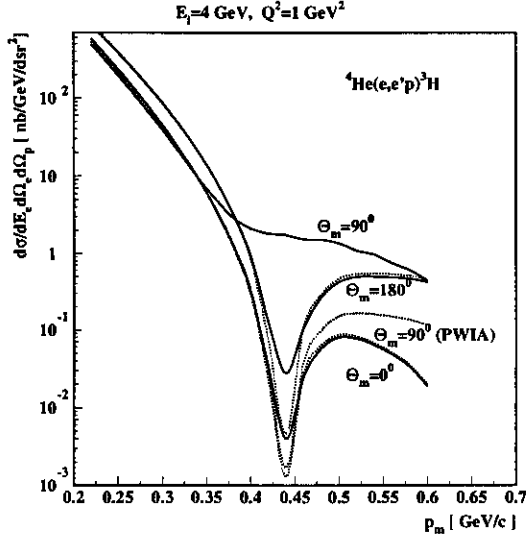


Figure 5: Cross sections for  ${}^4\text{He}(e, e'p){}^3\text{H}$  when the struck nucleon was travelling parallel ( $\Theta_m = 0^\circ$ ), perpendicular ( $\Theta_m = 90^\circ$ ), and antiparallel ( $\Theta = 180^\circ$ ) to the virtual photon.  $\Theta_m$  gives the angle that the struck nucleon's initial momentum makes with  $\vec{q}$ . The dashed curves are the PWIA calculations, and the solid curves include FSI.

### 3.3 Choice of $y$ Parameter

As explained above,  $y$  is the minimum momentum a struck nucleon must have had in order to satisfy the observed electron kinematics. Given the considerations in the previous section, it would seem obvious that if one wishes to minimize FSI contributions to a measured cross section at a given  $p_m$  value, one should choose  $y$  so that it is not significantly smaller than  $p_m$ . However, this is the same as saying “always measure near parallel kinematics” and so adds no new insight.

There is, however, additional information encoded in  $y$ :

- the sign of  $y$  indicates the direction in which a struck nucleon was moving before the collision; positive values of  $y$  indicates a nucleon moving in the same direction as the virtual photon, and negative  $y$  indicates an original motion opposite to the virtual photon's momentum vector.
- The sign and magnitude of  $y$  indicate the relation of the chosen electron

kinematics to the quasifree peak position. Positive  $y$  indicates an excess of energy transfer relative to the momentum transfer (the high-energy side of the quasielastic peak) while negative  $y$  indicates the opposite condition. The magnitude of  $y$  indicates how far off the peak the chosen kinematics are.

Selection of  $y = 0$  in parallel kinematics corresponds to knocking out an originally stationary nucleon. Cases have been made recently [25, 26, 27, 28] for the advantages of measuring at both positive and negative values of  $y$  in order to suppress reaction-mechanism effects such as FSI and MEC.

### 3.3.1 Positive $y$

In positive- $y$  kinematics there is an excess of energy transfer over momentum transfer (relative to the QE peak). In inclusive experiments, this is undesirable as reaction effects are seen to be larger at positive  $y$  values than when  $y \leq 0$ . However, for the special situation of  $(e, e'p)$  in parallel kinematics, positive  $y$  is thought to be advantageous since all of both  $\vec{q}$  and  $\vec{p}_s$  (the initial momentum of the struck nucleon) must go into the final ejected-proton momentum. Parallel kinematics coupled with positive  $y$  specifies that  $|\vec{p}_f| = |\vec{q}| + |\vec{p}_s|$ . Contaminating or multistep processes are suppressed since they can only contribute if they conspire to line up with  $\vec{q}$ .

Theoretical support for this argument is provided in a recent article [24] which examines FSI for  $A(e, e'p)$  reactions in a generalized eikonal approach (GEA). Minimal effects of FSI on the measured  $(e, e'p)$  cross sections are found when

$$\vec{p}_s \cdot \hat{q} > k_F, \quad (1)$$

where  $k_F$  is the usual Fermi momentum. We recall here that in parallel kinematics,  $y = \vec{p}_s \cdot \hat{q}$ .

### 3.3.2 Negative $y$

The qualitative argument for choosing to measure at negative values of  $y$  come from the inclusive experience mentioned earlier. Due to the smaller value of the energy transfer (relative to  $|\vec{q}|$ ), one expects MEC and  $\Delta$ -excitation effects to be smaller. On the other hand, detractors of this technique argue that since there are many ways for FSI or other effects to degrade the momentum of a struck proton, it is easy for them to produce cross section

at  $|\vec{p}_f| = |\vec{q}| - |\vec{p}_s|$ . The cross sections can be large if the strength which is being rescattered comes from lower- $|\vec{p}_s|$  components of the spectral function.

The generalized eikonal model makes a prediction about the contributions from FSI in negative- $y$  kinematics: FSI are expected to be small when

$$|\vec{p}_s \cdot \hat{q}| - E_m > k_F. \quad (2)$$

(Note here we take the absolute value of the inner product since the result is negative.) Since we are interested in the two-body breakup channel ( $E_m = 19.82$  MeV), this condition is essentially the same Eq. 1. Fig. 5 shows FSI are suppressed in both positive- $y$  ( $\Theta_m = 0$ ) and negative- $y$  ( $\Theta_m = 180^\circ$ ) kinematics, but the suppression is more effective at positive  $y$  values.

### 3.4 Effects of Variation of $Q^2$

The choice of the  $Q^2$  at which one measures may be important because of its impact on the contributions from non-nucleon degrees of freedom such as MEC and IC. To estimate the contribution from MEC, it is important to note that MEC diagrams have additional  $\sim 1/Q^2$  dependences compared to the diagrams where the electron scatters from a nucleon.

First, since at the considered kinematics the knocked-out proton is fast and takes almost the entire momentum of the virtual photon  $q$ , the exchanged meson propagator is proportional to  $(1 + Q^2/m_{\text{meson}}^2)$ . For purposes of estimation, we take  $m_{\text{meson}} = m_\rho$  (spin=1) since the  $\pi$  mesons exchange decreases much faster (because of spin=0).

Secondly, an additional  $Q^2$  dependence comes from the  $NN\rho$  formfactor  $\sim (1 + Q^2/\Lambda)$ . Thus overall additional dependence as compared to the PWIA diagram is [29]

$$\left( \frac{1}{(1 + Q^2/m_\rho^2)(1 + Q^2/\Lambda)} \right)^2, \quad (3)$$

where  $m_\rho = 0.71$  GeV and  $\Lambda \sim 0.8-1$ .

Note that we estimate only the contribution from the square of the MEC diagram - MEC will tend to fill the minimum of the  $n(p_m)$ . The contribution from the interference of MEC and PWIA amplitudes are suppressed even more since the PWIA diagram is vanishes where minimum occurs. Furthermore, the interference between the MEC and FSI amplitudes is suppressed by the real part of the FSI amplitude, which is a small correction for GeV rescattered nucleons.



Thus MEC make a mainly positive contribution to the cross section, and one can estimate this contribution using the results from NIKHEF measurement and rescaling factor from eq. 3. The NIKHEF measurements were performed at a  $Q^2$  of  $0.11 \text{ (GeV/c)}^2$ , while the measurements we are proposing have  $Q^2$  in the range  $0.8\text{--}1.9 \text{ (GeV/c)}^2$ . Thus we expect MEC effects to be suppressed by factors ranging from 10 to 100 in the kinematics discussed below.

To estimate the IC contribution, one note that in the considered  $Q^2$  range the  $\Delta$  transition form factor scales approximately as a elastic form factor[30]. Thus the only suppression comes from the virtualness of the intermediate  $\Delta$ 's. In this case IC contribution expressed through the single nucleon momentum dependence:

$$n \left( p_{mt}, p_{mz} - \frac{M_{\Delta}^2 - M_N^2}{2q} \right) \quad (4)$$

where  $p_{mt}$  and  $p_{mz}$  are the transverse and longitudinal components of the measured missing momentum. This equation shows the IC contribution will be stronger in  $+y$  region than for  $-y$  since in that case  $p_{mz} - \frac{M_{\Delta}^2 - M_N^2}{2q} < p_{mz}$ . As in the case of MEC, the IC will tend to fill the minimum, since its interference with PWIA and FSI will be suppressed following an argument similar to the one just presented for MEC.

## 4 Proposed Experiment

The experiment we propose to perform has two main goals:

1. to measure  $(e, e'p)$  cross sections across the minimum in  $n_{tp}(k)$  which are as closely related to the spectral function as possible. That is to say, we want to measure in kinematics where reaction-mechanism effects such as FSI, MEC, and IC are minimal.
2. to find out which of the proposed types of kinematics (as discussed in the previous section) actually result in minimal reaction-mechanism effects.

These two goals are obviously interrelated; if we don't succeed in finding a kinematic region in which FSI and other effects are sufficiently suppressed, we have no hope of achieving the first goal.

We propose to measure the relevant ( $e, e'p$ ) cross sections in two different kinematic types:

- constant ( $q, \omega$ ) (CQ $\Omega$ ) kinematics, in which  $\vec{q}$ ,  $\omega$ , and the relative energy between the ejected proton and recoil triton are kept constant;  $p_m$  is varied by changing the proton detection angle with respect to  $\vec{q}$ ;
- “+ $y$ ” (PY) kinematics, in which the proton is detected as closely parallel to  $\vec{q}$  as possible, and the recoil momentum  $p_m$  is varied by changing  $\omega$  (and thus  $|\vec{q}|$ ). The electron-scattering angle is kept fixed for simplicity. This means that the proton-detection angle must change with  $\omega$ .

We do not explicitly investigate “- $y$ ” kinematics, as this is the focus of approved experiment 97-011. However, the CQ $\Omega$  kinematics we have chosen happen to also have negative  $y$ .

All of the chosen kinematical settings involve momentum transfers in the range 0.9–1.7 GeV/ $c$ , since it is generally accepted that larger  $q$  is better for suppressing FSI. Furthermore, to address the question of contributions from MEC and IC, we measure at two different values of  $Q^2$  for each kinematic type, which according to the arguments of sec. 3.4 should change the MEC and IC contributions by a substantial factor.

Finally, the measurements are made over a rather wide range of  $p_m$ . In cases where no minimum is observed in this experiment, it is important to understand why. If measurements are made only over the region of interest, it will be impossible to draw any conclusions from a failure to see a minimum. Measurements for  $p_m < 350$  MeV/ $c$  give us data where we are more or less sure the calculations will find good agreement (see Fig. 4). Thus we can calibrate the calculations allow a better understanding of why the calculations don't work, in case they don't.

## 4.1 CQ $\Omega$ Kinematics

The NIKHEF data were measured in constant ( $q, \omega$ ) kinematics. Here the electron kinematics are fixed, and the recoil momentum is varied by detecting the ejected proton at different angles with respect to  $\vec{q}$ .

We propose to measure  $\sigma(p_m)$  in this type of kinematics. The main difference between our proposed setup and that of the NIKHEF data is that our  $|\vec{q}|$  setting is much larger, as are the outgoing proton momenta. The larger

CQ $\Omega$ electron kinematics			
Parameter	NIKHEF Data	CQ $\Omega$ I	CQ $\Omega$ II
Beam Energy (MeV)	525	4045	4045
Scattering Angle (deg)	49.6	14.17	20.88
Energy Transfer (MeV)	215	400	530
$ \vec{q} $ (MeV/c)	401	1028	1466
$Q^2$ (GeV/c) <sup>2</sup>	0.11	0.90	1.87
$y$ (MeV/c)	220	-105	-400
$\theta_q$ (deg)	36.07	60.21	58.73

Table 1: Summary of  $(e, e')$  kinematics for NIKHEF data and the proposed CQ $\Omega$  measurements.

momenta should reduce FSI contributions. Two sets of measurements will be made, corresponding to two different values of  $Q^2$ . Comparison of the two sets should give some information on the amount of subnucleonic strength (MEC and IC) present, and on how well the calculations are treating these effects.

The proposed kinematics are displayed in Tables 1 and 2. Table 1 also includes the kinematics for the NIKHEF experiment for comparison. We also present calculations for the expected cross sections which have been computed in the GEA discussed earlier. Fig. 6 shows a comparison of the results of this calculation to the NIKHEF data. This comparison should be viewed as qualitative, since the calculation is based on approximations which begin to fail for  $Q^2 < 1$  (GeV/c)<sup>2</sup>. The NIKHEF data were acquired at  $Q^2 = 0.11$  (GeV/c)<sup>2</sup>. The GEA calculations do not at present include contributions from MEC or IC. The results of the full GEA calculation are qualitatively similar to those of Schiavilla when no MEC are included (dashed curve in (panel b) of Fig. 4).

Fig. 7 shows calculations for the expected results of the current proposal's CQ $\Omega$  I ( $Q^2 = 0.9$  (GeV/c)<sup>2</sup>) and CQ $\Omega$  II ( $Q^2 = 1.9$  (GeV/c)<sup>2</sup>) kinematical settings. Note that in the CQ $\Omega$  I kinematical setting, we take additional data on the  $(e, e'p)$  cross section for recoil momenta as low as 100 MeV/c. For this region, we are certain that PWIA will play a dominant role, allowing unambiguous comparison with all previous measurements and with calculations. The calculations shown in the figure predict that the CQ $\Omega$  I

CQ $\Omega$ Detector Settings			
$p_m$	$p_{\text{cent}}^{\text{HRSh}}$	$\theta_p$	$p_p$
(MeV/c)	(MeV/c)	(deg)	(MeV/c)
CQ $\Omega$ I Measurement			
106.4	908.7	-61.3	923.4
356.0	908.7	-80.0	894.0
434.8	868.5	-85.0	878.0
512.4	868.5	-90.0	859.0
CQ $\Omega$ II Measurement			
400.1	1059	-59.5	1066.0
425.9	1059	-64.8	1061.0
468.7	1059	-68.9	1052.0
562.1	1029	-75.3	1029.3

Table 2: Hadron-arm kinematics for CQ $\Omega$  I and CQ $\Omega$  II measurements. Values given are for the center of the acceptances.

measurement will make little improvement upon the existing data, but the CQ $\Omega$  II kinematics show little effect from FSI.

The source of the improvement of CQ $\Omega$  II *vs.* CQ $\Omega$  I with respect to FSI is difficult to identify. The possible culprits are:

- proton momentum increase: 1052 MeV/c (II) *vs.* 878 MeV/c (I);
- parallelness:  $\theta_{pq} = 10.2$  deg (II) *vs.* 24.8 deg (I);
- struck-nucleon momentum  $z$ -component (see Sec. 3.3.2): -430 MeV/c (II) *vs.* -230 MeV/c (I).

All numbers quoted are for  $p_m \sim 450$  MeV/c.

## 4.2 PY Kinematics

This part of the proposed measurement plan exploits all but one of the techniques listed in section 3 which are thought to suppress FSI and MEC.

- Large values (900–1700 MeV/c) of  $|\vec{q}|$  are used.
- All measurements are made in parallel kinematics.

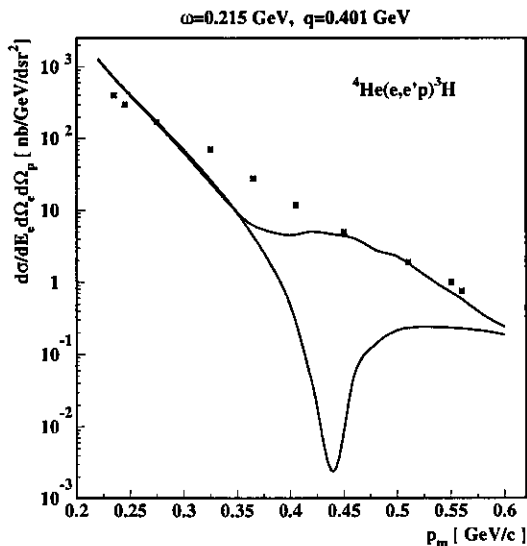


Figure 6: Cross sections for  ${}^4\text{He}(e, e'p){}^3\text{H}$  measured at NIKHEF. The dashed curve is a PWIA calculation. The solid curve includes FSI in the approximations of the GEA. Other effects such as MEC and IC are not included. The calculation should be viewed as illustrative since the NIKHEF kinematics fall outside the range of validity of the GEA.

- Positive values of  $y$  are chosen (sec. 3.3.1).
- measurements are made in two different regimes of  $Q^2$  (sec. 3.4).
- Since all measurements are made in parallel kinematics, the  $z$  component of the struck nucleon momentum is ensured to satisfy eq. 1.

Table 3 displays the chosen kinematical settings. Figure 8 shows the predicted results calculated in the GEA. The minimum in the spectral function is preserved in both cases. One puzzling feature is that the minimum is better preserved in PY-I than in PY-II, and the CQ $\Omega$ -II calculation shows better preservation of the minimum than either of the PY settings. This is contrary to expectations based on the qualitative arguments presented in Sec. 3, and it will be interesting to see how the calculation fares against reality.

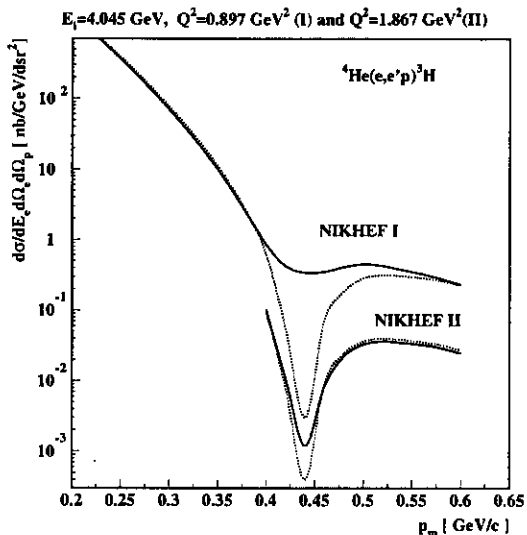


Figure 7: Calculated cross sections for  ${}^4\text{He}(e, e'p){}^3\text{H}$  in the CQ $\Omega$  I and CQ $\Omega$  II kinematics of the current proposal. The dashed curves are PWIA calculations, and the solid curves include FSI in the GEA.

## 5 Experimental Considerations

We propose to perform the experiment in Hall A. The high-resolution spectrometer pair is well suited to the task at hand. Large acceptances are not necessary since we measure on the two-body breakup channel, and in the case of the PY kinematics, large angular acceptances are even undesirable. The HRS pair can be operated in a standard configuration for this experiment.

The only nonstandard equipment necessary is the High-Power Helium Cryotarget (HPHC). The present end-station refrigerator at Jefferson Lab has insufficient cooling power to run the HPHC unless one of the other halls is down or is running without some of the standard cryogenically-cooled equipment. This means that Hall A experiments using the HPHC will tend to be lumped together, thus we do not treat the necessary installation time for the HPHC as part of this proposal.

PY Kinematics Summary					
$\omega$	$ \vec{q} $	$p_m$	$p_e$	$p_p$	$\theta_p$
(MeV)	(MeV/c)	(MeV/c)	(MeV/c)	(MeV/c)	(deg)
PY kinematics I					
Beam Energy 2445 MeV, $\theta_e = 16.83$ deg					
650	893.6	337.9	1795	1231.5	-35.6
850	1027.9	432.0	1595	1459.9	-26.7
1050	1181.0	499.2	1395	1680.2	-20.0
PY kinematics II					
Beam Energy 3245 MeV, $\theta_e = 18.78$ deg					
1000	1332.6	320.0	2245	1652.5	-32.8
1300	1536.9	436.2	1945	1973.1	-24.0
1500	1689.1	493.3	1745	2182.3	-19.4

Table 3: Summary of kinematics and detector settings for PY measurements. Values given are for the center of the acceptances.

## 5.1 Count Rate Estimates

The calculations shown in this proposal indicate that the expected cross sections are in most cases roughly equal to those predicted by the PWIA, except near the minimum where they are factors of 2–100 times larger, depending on the kinematics. We thus use the PWIA as a guide in estimating the required beam times.

These estimates were generated using the Monte-Carlo code AEEXB [31]. Spectrometer parameters (angular and momentum acceptances) were taken from the CDR. The following parameters were used for the HPHC [32]:

- length along beam direction: 10 cm;
- target density: 0.1525 g/cm<sup>3</sup>;
- maximum beam current: 100  $\mu$ A.

The Monte-Carlo calculation results were then scaled so that the histograms read in units of counts per 100  $\mu$ A-hr. Figures 9 thru 13 show the predicted count rates in PWIA for all the kinematic settings listed in the proposal. These count rates do not account for the acceptance function of the

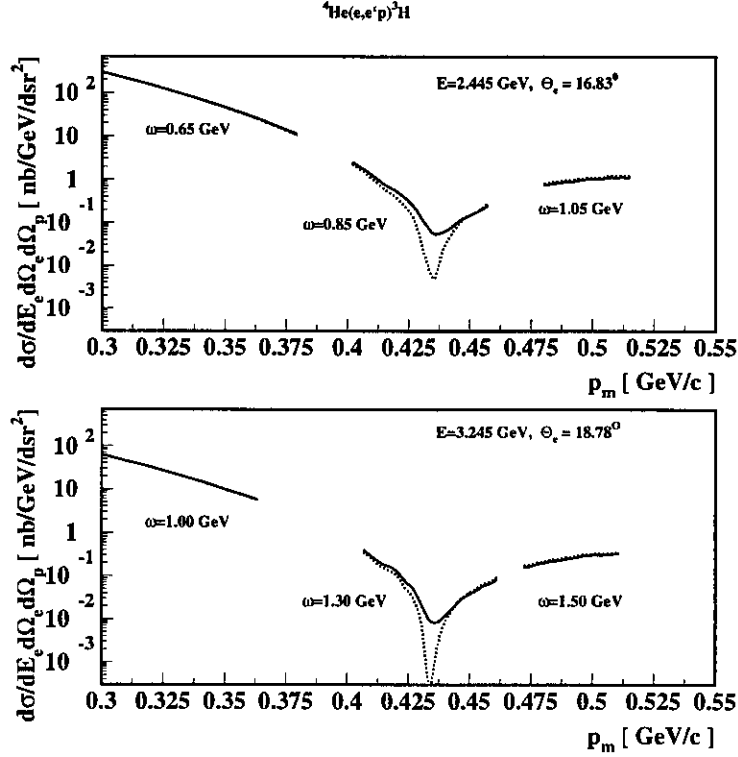


Figure 8: Calculated cross sections for  ${}^4\text{He}(e, e'p){}^3\text{H}$  in the PY I and II kinematics of the current proposal. The dashed curves are PWIA calculations, and the solid curves include FSI in the GEA. The six curve segments shown correspond to the six distinct PY subsettings, varying  $\omega$  by the limits imposed on the spectrometer momentum bite within each subsetting.

spectrometers in the  $y_{\text{tgt}}$  coordinate (the displacement of an event from the spectrometer vertex along the beam direction, projected onto a plane perpendicular to the spectrometer's central ray). This point will be discussed again shortly. The bin size in  $p_m$  is 10 MeV/c.

One might be concerned about the large degree of overlap in the  $p_m$  range covered by the various kinematic settings within each subprogram. The large range stems from the large momentum acceptances (and to a lesser extent, the angular acceptances) of the HRS pair. In order to properly explore the ideas put forward in this proposal, it will be necessary to use data from each of the settings. This is especially true for the CQ $\Omega$  kinematics, where the



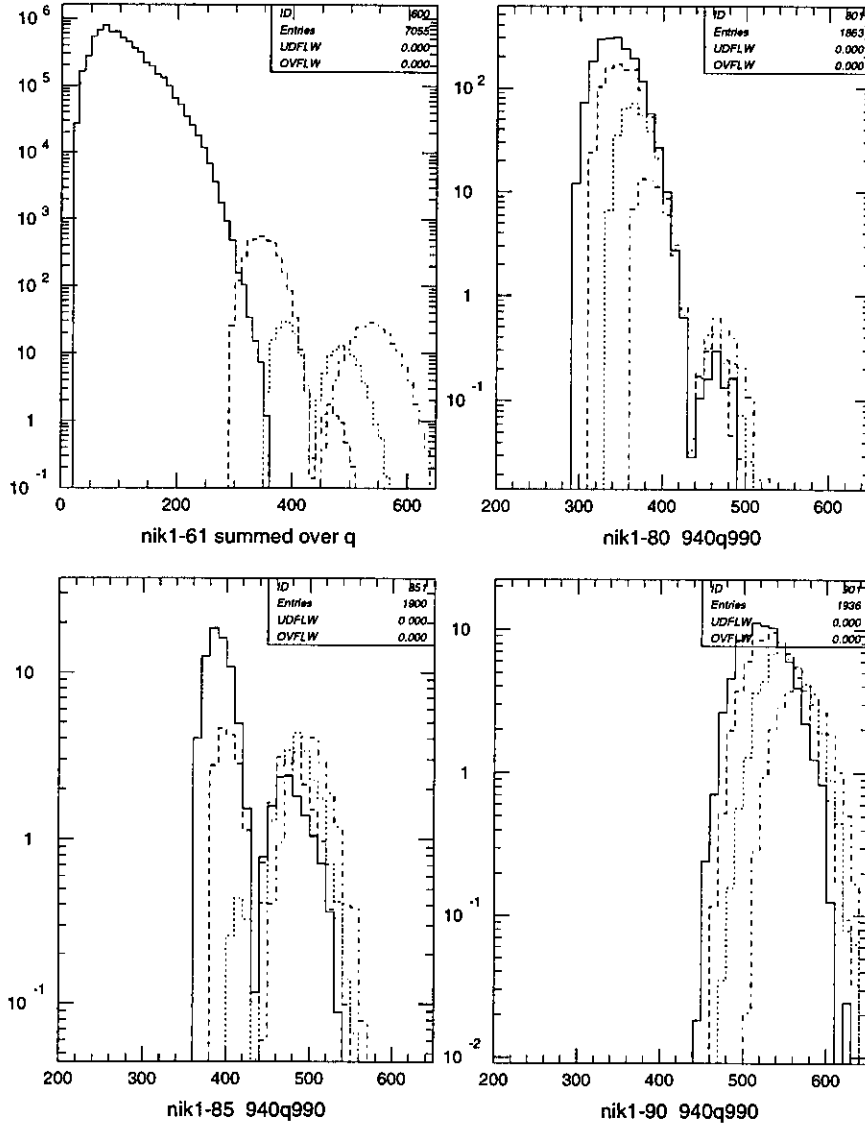


Figure 9: Simulated results for CQΩ I kinematics. The vertical axis has units counts per 100  $\mu\text{A-hr}$ . Upper Left (UL) Panel: rates for all four settings, no cuts applied. Upper Right (UR) Panel: rates for  $\theta_p = 80$  deg setting. Lower Left (LL) Panel: rates for  $\theta_p = 85$  deg setting. Lower Right (LR) Panel: rates for  $\theta_p = 90$  deg setting. The last three panels display four overlaid histograms, each of which corresponds to a different bite in  $|\vec{q}|$ .

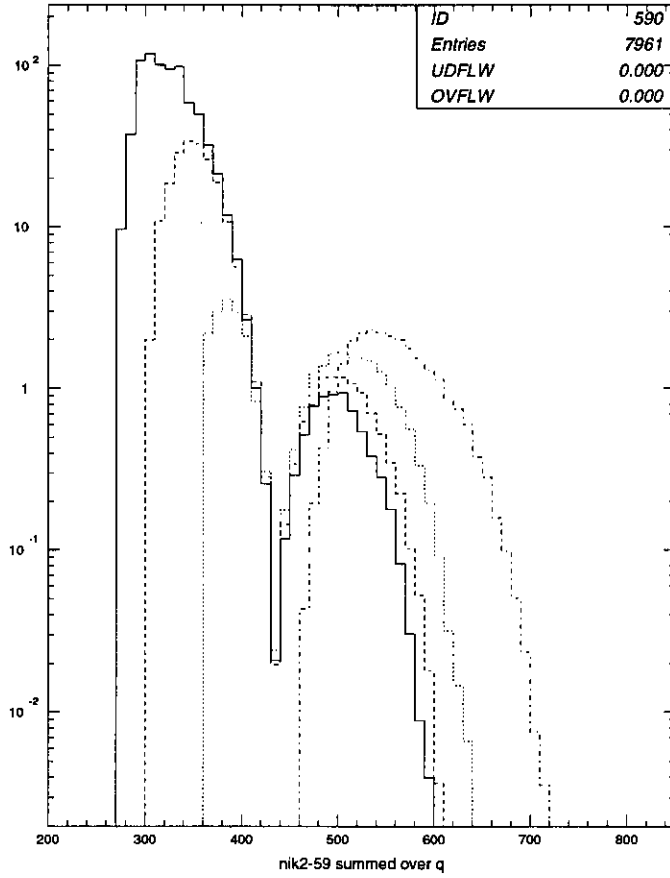


Figure 10: Simulated results for CQ $\Omega$  II kinematics. The vertical axis has units counts per 100  $\mu$ A-hr. Four curves are shown, which are the results for the four different settings of  $\theta_p$  with no cuts applied.

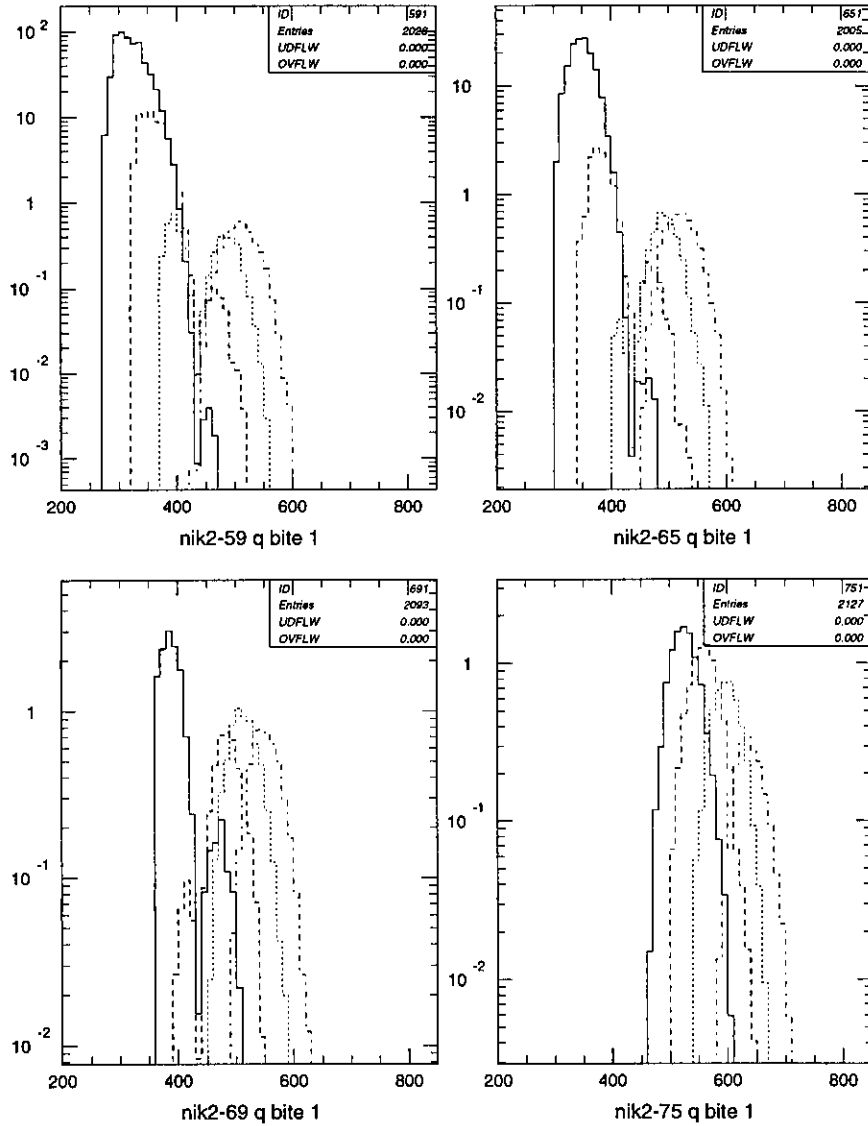


Figure 11: Simulated results for CQΩ II kinematics. The vertical axis has units counts per 100  $\mu\text{A-hr}$ . Upper Left (UL) Panel: rates for  $\theta_p = 59.5$  deg setting. Upper Right (UR) Panel: rates for  $\theta_p = 64.8$  deg setting. Lower Left (LL) Panel: rates for  $\theta_p = 68.9$  deg setting. Lower Right (LR) Panel: rates for  $\theta_p = 75.3$  deg setting. The panels display four overlaid histograms, each of which corresponds to a different bite in  $|\vec{q}|$ .

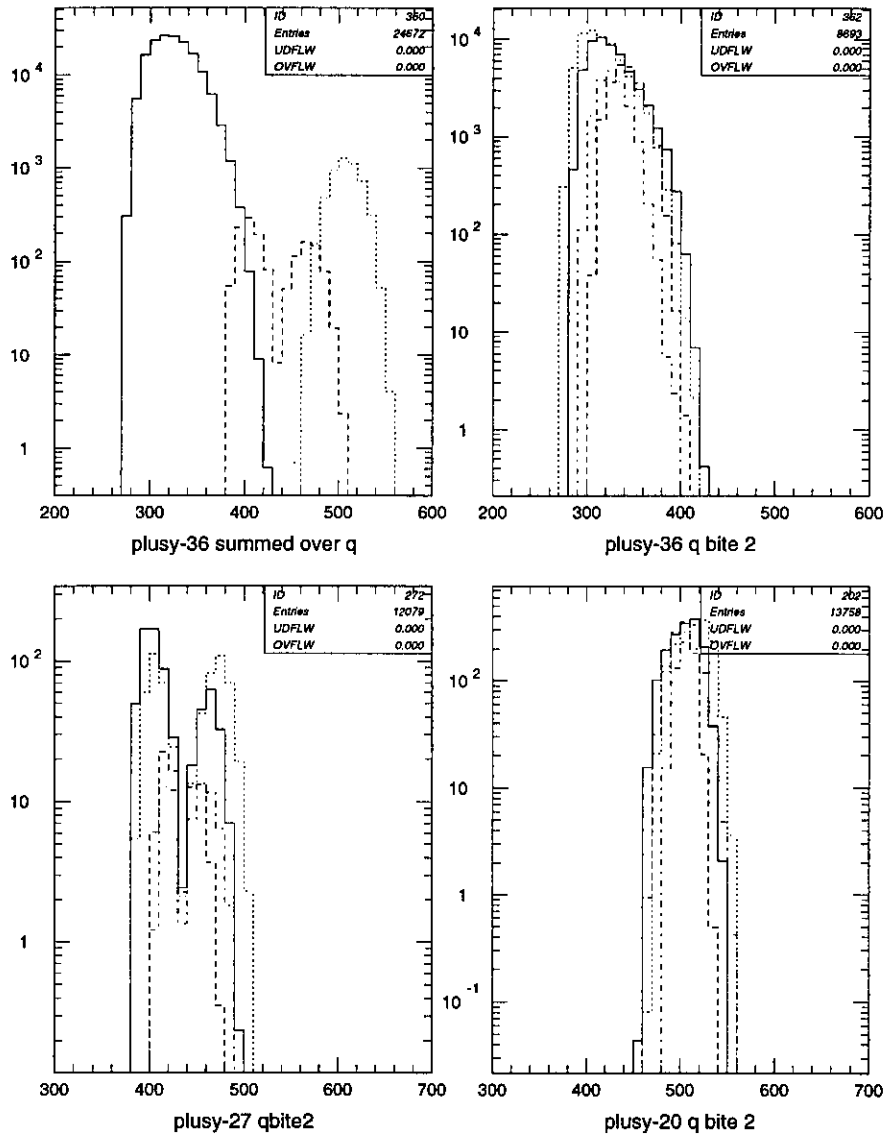


Figure 12: Simulated results for PY I kinematics. The vertical axis has units counts per 100  $\mu\text{A-hr}$ . Upper Left (UL) Panel: rates for all three settings overlaid, with no cuts applied. Upper Right (UR) Panel: rates for  $\omega = 650$  MeV setting. Lower Left (LL) Panel: rates for  $\omega = 850$  MeV setting. Lower Right (LR) Panel: rates for  $\omega = 1050$  MeV setting. The panels display four overlaid histograms, each of which corresponds to a different bite in  $|\vec{q}|$ .

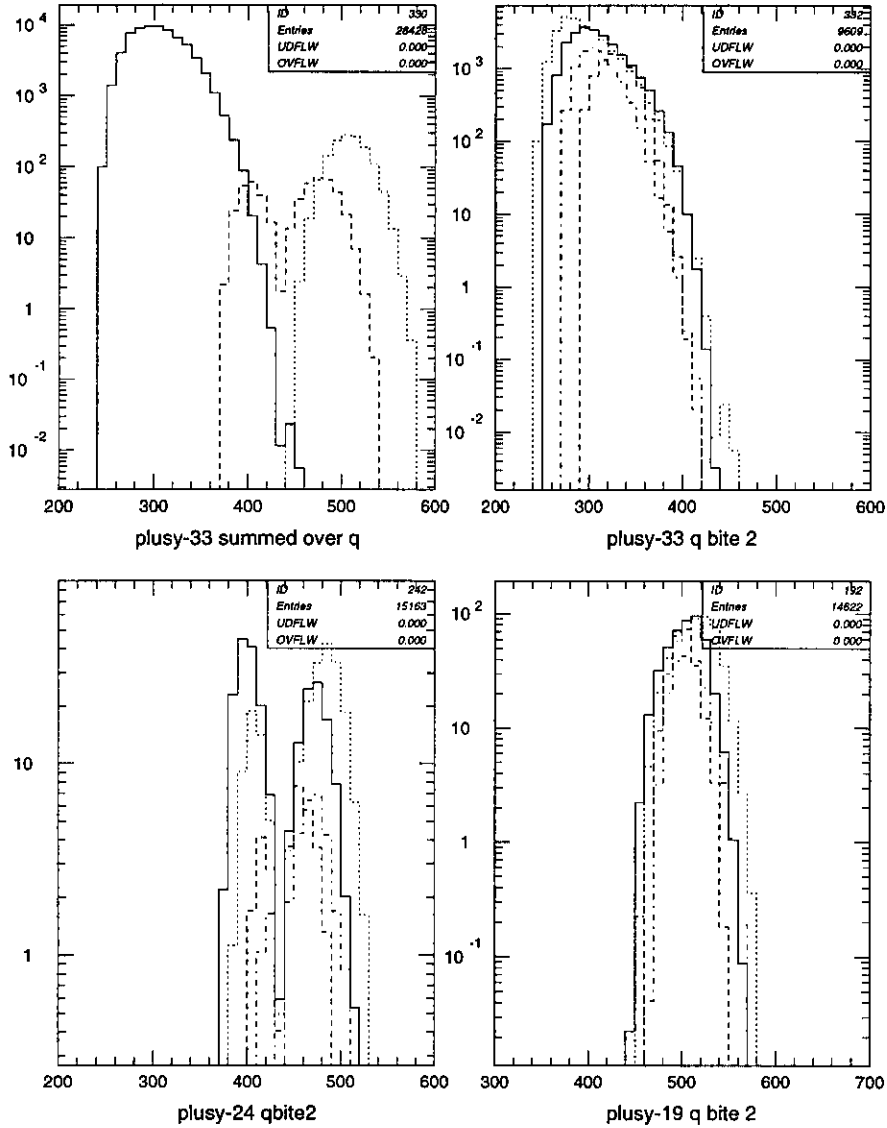


Figure 13: Simulated results for PY II kinematics. The vertical axis has units counts per  $100 \mu\text{A}\cdot\text{hr}$ . Upper Left (UL) Panel: rates for all three settings overlaid, with no cuts applied. Upper Right (UR) Panel: rates for  $\omega = 1000$  MeV setting. Lower Left (LL) Panel: rates for  $\omega = 1300$  MeV setting. Lower Right (LR) Panel: rates for  $\omega = 1500$  MeV setting. The panels display four overlaid histograms, each of which corresponds to a different bite in  $|\vec{q}|$ .

main feature we wish to test is the effect of variation of  $\theta_{pq}$  on the final-state interactions. This is somewhat less of a point with the PY kinematics, but there the overlap is between settings is considerably less.

## 6 Beam Time Request

Assuming that the cryotarget parameters used realistically reflect those of the real target, and that we can run at a beam current of  $100 \mu\text{A}$ , the simulation figures read off in counts per hour per 10 MeV/c bin of  $p_m$ . Based on these numbers, we construct the beam time estimate for the experiment in hours. We are guided by the following considerations:

- where the count rate is very high, we take a measurement for one hour;
- where the count rate is large but not very high, we adjust the beam time to get about 3% statistics (1000 counts) for those bins with the highest counting rates in the setting;
- where the count rate is very low, we adjust the beam time to get at least 20% statistics (25 counts) for those bins with the highest counting rates in the setting
- in each setting except for CQ $\Omega$ I, we try to make a 10% measurement for the two points bracketing the minimum in the computed cross section. We relax this requirement for the CQ $\Omega$  II kinematics, where we would need to count for on the order of 500 hours if we trust the PWIA.
- the estimates are based on the simulation results after application of cuts. It is clear that cuts will need to be applied to the data, given the large acceptances involved. It is not clear that the cut used (selecting four different slices in  $|\vec{q}|$  for each setting) is the best one. We have also not adjusted the counting-rate estimates based on the observation that the minima are usually filled in by a factor ranging from five to one hundred; we prefer to be conservative in trimming beam time, which allows us to make more aggressive cuts in the final data set.

The requested beam time for production measurements is shown in table 4. The numbers have been adjusted for the spectrometer acceptances in  $y_{\text{tgt}}$  according to a recent measurement [33]. The FWHM of the spectrometer

$y_{\text{tgt}}$  acceptance was found to be 7 cm, while the HPHC has a full length of 10 cm.

Production Measurement Time Request		
Kinematic Type	Detector Setting	Time (hr)
CQ $\Omega$ -I	$\theta_p = 61.3$ deg	2
CQ $\Omega$ -I	$\theta_p = 80.0$ deg	9
CQ $\Omega$ -I	$\theta_p = 85.0$ deg	18
CQ $\Omega$ -I	$\theta_p = 90.0$ deg	18
CQ $\Omega$ -II	$\theta_p = 59.5$ deg	19
CQ $\Omega$ -II	$\theta_p = 64.8$ deg	38
CQ $\Omega$ -II	$\theta_p = 68.9$ deg	38
CQ $\Omega$ -II	$\theta_p = 75.3$ deg	38
"PY"-I	$\omega = 650$ MeV	1.5
"PY"-I	$\omega = 850$ MeV	13
"PY"-I	$\omega = 1050$ MeV	13
"PY"-II	$\omega = 650$ MeV	1.5
"PY"-II	$\omega = 850$ MeV	27
"PY"-II	$\omega = 1050$ MeV	13
<b>TOTAL</b>		<b>249</b>

Table 4: Times required for the measurement at each setting, as estimated from the Monte-Carlo simulations.

## 6.1 Other Beam Time

We request the following additional time for performing the experiment:

- at each beam energy, one hour for performing sieve-slit checks of the spectrometer optics (**total: 3 hr**)
- at each beam energy, two hours for performing  ${}^1\text{H}(e, ep)$  calibrations (**total: 6 hr**)
- at each beam energy, four hours for changing over from hydrogen gas to helium gas. The switch from helium to hydrogen can be made concurrently with a beam-energy change, so no time is asked for that process (**total: 12 hr**)

- 10 spectrometer angle changes (**total: 10 hr**). Magnetic-field changes always happen in conjunction with some other change for which we have asked time, so no extra time is needed for magnet changes.

The sum total of this additional time is **31 hr**. We also request eight hours time with no beam, before the experiment is started. In this time we'd like to double-check the spectrometer angular positions by survey techniques.

The total beam-on time discussed above amounts to **280 hr**.

## 7 Relation to other Jefferson Lab Approved Experiments

There are several experiments in the general area of  $(e, e'p)$  spectral-function studies, which plan to make an attempt to find how to reduce FSI or MEC contributions, or to measure short-range correlations. Our proposal is unique in several ways:

- it is the only proposal which emphasizes the physics of SRC in the two-body breakup spectral function of  ${}^4\text{He}$ ;
- it is the only one in which both PY and  $-y$  settings are tested for suppression of FSI effects;
- it requires less running time than the other experiments, since ours is optimized for this specific study on the two-body breakup channel.

We now discuss each of these other experiments in turn.

### 7.1 Expt. 89-044

This proposal includes a broad program of study on the reaction  ${}^3\text{He}(e, e'p)$ . The proposal to the PAC also requested time for studies on  ${}^4\text{He}$ , but this part was not approved. The study is divided into three parts:

- Part I: two-body breakup measurements in perpendicular kinematics, with structure-function separations.
- Part II: studies of the  $Q^2$  dependence of the longitudinal and transverse response functions for two-body breakup (in parallel kinematics).



- Part III: measurements for continuum breakup reactions with structure-function separations.

Only part I of 89-044 has a significant overlap with the physics of the current measurement. The first  $Q^2$  point of 89-044 lies below that of the current CQ $\Omega$ -I kinematics (0.55 *vs.* 0.90 (GeV/c)<sup>2</sup>), and should be even more sensitive to FSI since  $\theta_{pq}$  is large ( $> 30$  deg) for the high- $p_m$  kinematics. The second  $Q^2$  point of part I of 89-044 has some similarities to our CQ $\Omega$ -II kinematics, although the 89-044 kinematics have  $y = 0$  and large  $\theta_{pq}$ , so one would not expect a significant suppression of FSI at high  $p_m$  based on the arguments in this proposal. Thus part I of 89-044 is not competitive with the current proposal. Part II of 89-044 carries our exploration of the  $Q^2$ -dependence of reaction-mechanism effects much further, but it is limited to  $p_m \leq 300$  MeV/c.

## 7.2 Expt. 97-006

Experiment 97-006 studies how reaction-mechanism effects (especially FSI) affect the measurement of nuclear hole spectral functions. This study will cover a large kinematic range and study several nuclei. Some of the kinematical settings in that proposal (particularly settings 4 and 5) have some overlap with the PY settings of the current proposal, although those for 97-006 have lower  $Q^2$ .

The philosophy of 97-006 with respect to minimizing FSI was partially responsible for inspiring the PY measurements of the current proposal, thus there is quite definitely much in common here. However, 97-006 is optimized for measurements at deep ( $> 50$  MeV) missing energy, and <sup>4</sup>He is not one of the chosen targets.

## 7.3 Expt. 97-011

This experiment is aimed at measurements of <sup>3,4</sup>He( $e, e'p$ ) in parallel kinematics at large negative  $y$ . It is optimized for measurement at deep missing energy, but the two-body breakup peak is within the acceptance. There is a strong overlap between the 97-011 point at  $Q^2 = 2$  (GeV/c)<sup>2</sup>,  $y = -450$  MeV/c, and our proposal's CQ $\Omega$  II kinematics. There are no other significant overlaps, and in particular there are no PY settings in 97-011, and no data for  $p_m > 450$  MeV/c, rendering verification of a minimum or observation of

a second maximum virtually impossible. Expt. 97-011 is primarily aimed at measurement of the continuum spectral function, so the physics-goal overlap is small.

#### 7.4 Expt. A1/3-96 at Mainz

While this experiment is performed elsewhere, there is significant physics overlap with 97-011 and a slight overlap with the goals of the current proposal. The experiment studies the  $y$ -dependence of the longitudinal and transverse response functions for  ${}^3,4\text{He}(e, e'p)$ . However, the study of  $y$  dependence is made in the context of possible MEC and IC contributions to the transverse response at high  $E_m$ . The chosen values of  $y$  are small ( $< 200 \text{ MeV}/c < k_F$ ) and thus are probably too low to have a large effect on FSI. The experiment covers a large (150 MeV) range of missing energy. Data on the two-body breakup are acquired as well, but the acceptance is limited to  $p_m < 300 \text{ MeV}/c$  for this channel. Thus this experiment will gain no information on SRC structure in the  $pt$  momentum distribution.

## 8 Conclusions

Modern, sophisticated calculations of the structure of  ${}^4\text{He}$  and the associated spectral function for proton removal to the triton ground state, make a definite prediction of a minimum and maximum in the spectral function in the region between 350 and 500 MeV/ $c$ . The predictions further associate this structure with  $s$ -wave components, which explicitly emphasize the shorter-range correlations. This structure has never been observed, and determining whether it is present is an important test of both the calculations as well as our understanding of the short-range  $NN$  interaction. Determining the location of the minimum and the height of the maximum will provide a further quantitative test of the various  $NN$  interaction models.

The proposed experiment will measure cross sections in the region of the predicted structure, in several different types of kinematics. The choice of the kinematics is designed to control various obscuring contributions such as FSI and MEC. Calculations predict that the FSI contributions will be reduced to a level where the minimum and maximum can be observed. The various kinematics are predicted to be quite different in their sensitivity to meson-exchange currents. Combining the results for the same region of  $p_m$

for the various kinematics will allow definite statements to be made about the spectral function minimum and maximum, as well as about the efficiency of suppression of FSI, MEC, and IC.

## References

- [1] Jefferson Lab PAC12 Report, 1997.
- [2] I. Bobeldijk et al., Phys. Rev. Lett. **73**, 2685 (1994).
- [3] K. I. Blomqvist et al., Phys. Lett. B **344**, 85 (1995).
- [4] I. Bobeldijk et al., Phys. Lett. B **353**, 32 (1995).
- [5] R. W. Lourie et al., Phys. Rev. Lett. **56**, 2364 (1986).
- [6] P. E. Ulmer et al., Phys. Rev. Lett. **59**, 2259 (1987).
- [7] C. Marchand et al., Phys. Rev. Lett. **60**, 1703 (1988).
- [8] J. M. Le Goff et al., Phys. Rev. C **50**, 2278 (1994).
- [9] J. J. van Leeuwe, *Investigation of Nucleon-Nucleon Correlations in  $^4\text{He}$* , PhD thesis, Universiteit Utrecht, 1996.
- [10] S. Tadokoro, T. Katayama, Y. Akaishi, and H. Tanaka, Prog. Theor. Phys. **78**, 732 (1987).
- [11] H. Morita, Y. Akaishi, and H. Tanaka, Prog. Theor. Phys. **79**, 863 (1988).
- [12] R. Schiavilla, V. Pandharipande, and R. Wiringa, Nucl. Phys. **A449**, 219 (1986).
- [13] H. Morita, Y. Akaishi, O. Endo, and H. Tanaka, Prog. Theor. Phys. **78**, 1117 (1987).
- [14] O. Unal et al., manuscript in preparation .
- [15] J. F. J. van den Brand et al., Phys. Rev. Lett. **60**, 2006 (1988).
- [16] J. F. J. van den Brand et al., Nucl. Phys. **A534**, 637 (1991).

- [17] J. F. J. van den Brand et al., Phys. Rev. Lett. **66**, 409 (1991).
- [18] J. E. Ducret et al., Nucl. Phys. **A556**, 373 (1993).
- [19] J. M. Laget, Nucl. Phys. **A579**, 333 (1994).
- [20] R. Schiavilla, Phys. Rev. Lett. **65**, 835 (1990).
- [21] S. I. Nagorny et al., Sov. J. Nucl. Phys. **49**, 465 (1989).
- [22] S. I. Nagorny et al., Sov. J. Nucl. Phys. **53**, 228 (1991).
- [23] A. Bianconi and M. Radici, Phys. Lett. B **363**, 24 (1995).
- [24] L. L. Frankfurt, M. M. Sargsian, and M. I. Strikman, Phys. Rev. C **56**, 1124 (1997).
- [25] Studies of the  $(e, e'p)$  reaction at high missing energy, MAMI Proposal A1/1-93, 1993.
- [26] Addendum to Proposal A1/1-93, Submitted to the MAMI PAC, 1994.
- [27] Correlated spectral function and  $(e, e'p)$  reaction mechanism, Jefferson Lab Proposal 97-006, 1997.
- [28] Initial exploration of semi-inclusive scattering in  $x > 1$  region  ${}^{3,4}\text{He}(e, e'p)$  reactions, Jefferson Lab Proposal 97-011, 1997.
- [29] D. O. Riska, Phys. Rep. **181**, 207 (1989).
- [30] P. Stoler, Phys. Rep. **226**, 103 (1993).
- [31] C. Vellidis, AEEXB: A Program for Monte Carlo Simulations of coincidence electron-scattering experiments, Technical Report to the OOPS Collaboration, MIT-Bates Accelerator Laboratory, 1997.
- [32] J.-P. Chen, private communication, 1997.
- [33] N. Liyange, private communication, 1997.